

Enhanced adhesion in two-photon polymerization direct laser writing

Cite as: AIP Advances 10, 045217 (2020); <https://doi.org/10.1063/5.0005548>

Submitted: 24 February 2020 . Accepted: 19 March 2020 . Published Online: 10 April 2020

A. G. Izzard, E. P. Garcia, M. Dixon, E. O. Potma , T. Baldacchini , and L. Valdevit



View Online



Export Citation



CrossMark



NEW

AVS Quantum Science

A new interdisciplinary home for impactful quantum science research and reviews

Co-Published by



NOW ONLINE



Enhanced adhesion in two-photon polymerization direct laser writing

Cite as: AIP Advances 10, 045217 (2020); doi: 10.1063/5.0005548

Submitted: 24 February 2020 • Accepted: 19 March 2020 •

Published Online: 10 April 2020



View Online



Export Citation



CrossMark

A. G. Izard,¹ E. P. Garcia,² M. Dixon,³ E. O. Potma,²  T. Baldacchini,^{2,4,a)}  and L. Valdevit^{1,5}

AFFILIATIONS

¹Mechanical and Aerospace Engineering Department, University of California, Irvine, California 92697, USA

²Department of Chemistry, University of California, Irvine, California 92697, USA

³Nanoscience Instruments, Inc., Phoenix, Arizona 85044, USA

⁴Schmid College of Science and Technology, Chapman University, Orange, California 92866, USA

⁵Materials Science and Engineering Department, University of California, Irvine, California 92697, USA

^{a)} Author to whom correspondence should be addressed: tbaldacc@uci.edu

ABSTRACT

We have quantified the adhesion forces between two-photon polymerization direct laser writing (TPP-DLW) microstructures and glass surfaces with and without an adhesion promoter. Glass surfaces treated with an acryloxy-silane agent produce adhesion forces that are almost three times larger than the forces observed with pristine glass surfaces. Determination of the substrates' surface free energies suggests that the observed adhesion enhancement is chemical in its nature, implying that covalent bonds are formed between the polymer and the glass by means of the silane agent. The importance of this finding is demonstrated in the successful production of glassy carbon microstructures using TPP-DLW, followed by pyrolysis.

© 2020 Author(s). All article content, except where otherwise noted, is licensed under a Creative Commons Attribution (CC BY) license (<http://creativecommons.org/licenses/by/4.0/>). <https://doi.org/10.1063/5.0005548>

I. INTRODUCTION

Two-photon polymerization direct laser writing (TPP-DLW) has the distinctive ability to print complex 3D microstructures with feature sizes that can reach dimensions as small as 100 nm.^{1–4} Over the years, this characteristic has propelled TPP-DLW into becoming an enabling technology for a wide range of applications. While the first examples focused exclusively on creating small and proof-of-concept structures,⁵ TPP-DLW has now matured into an additive manufacturing process capable of accelerating research in fields as diverse as photonics,^{6,7} mechanics,^{8,9} biology,^{10–12} medicine,^{13,14} and microfluidics.^{15–17} The adoption of TPP-DLW by a broad range of scientific disciplines is a consequence of its true 3D writing capability; the presence of both chemical and optical nonlinearities during TPP-DLW allows for the confinement of polymerization within sub-femtoliter volumes (voxels), hence achieving remarkably accurate printing performances.¹⁸ Voxels with lateral and axial dimensions of 200 nm and 500 nm, respectively, are commonly employed in TPP-DLW to print 2.5D and 3D patterns that can range in overall

part size from micro- to mesoscale.^{19,20} One of the applications that underlines the favorable qualities of TPP-DLW in microfabrication is the realization of mechanical metamaterials.²¹ Parts with effective material properties previously impossible to reach in monolithic systems are now routinely fabricated by TPP-DLW in conjunction with post-writing procedures such as atomic layer deposition and pyrolysis.^{22,23}

Although TPP-DLW is a thriving microfabrication technique when it comes to the fast prototyping of parts that are either impossible or too expensive/time-consuming to make with conventional methods, it still suffers from a number of limitations that hinder broader implementation.²⁴ Given that effects such as degree of conversion, solvent permeation, voxel overlap strategies, material inhomogeneities, and adhesion with different materials are poorly understood when polymerization is confined at the nanoscale, writing by TPP-DLW largely remains an empirical process.²⁵ This is particularly true when fabricating microstructures based on novel designs and/or new materials. A case in point is the strong and durable adhesion between polymeric microstructures and the substrate (in most

cases, a glass slide or a silicon wafer), which is essential for successful writing in TPP-DLW. The reliability of three-dimensional microfabrication is indeed strongly related to anchoring polymeric microstructures to solid substrates. Survivability and reproduction fidelity of complex three-dimensional parts critically depend on this bond.

Following this requirement, the TPP-DLW strategy commonly starts with finding the resin/substrate interface and then ensuring that printing is originated at this location. Auto-focusing modules are routinely implemented to assist in these tasks. Nonetheless, partial or complete detachment of printed parts still occurs, which is especially limiting when carrying out long print jobs. The causes of this failure point to the polymer swelling and shrinkage that evolve during and after fabrication.²⁵ In this article, we examine this important issue by measuring the force required to dislodge polymeric microstructures fabricated by TPP-DLW on several substrates. We find that the use of an acryloxy-based silane adhesion promoter can substantially increase the adhesion between the printed part and the substrate.

II. METHODS

TPP is performed using a Photonic Professional GT (Nanoscribe GmbH) DLW system equipped with a 63×1.4 NA microscope objective. The polymeric microstructures are printed on glass substrates from an acrylic-based resin (IP-Dip, Nanoscribe GmbH) in a layer-by-layer sequence using the system's galvanometric mirror scanning mode.²⁶ To ensure that the polymeric microstructures are anchored to the substrate, we followed the common procedure to set the first printed layer 1 μm below the resin/substrate interface as it is found by means of the system auto-focusing module.

After DLW, the unsolidified portion of the resin is washed away using a propylene glycol monomethyl ether acetate bath for 20 min, followed by a 5 min dip in isopropanol. The samples are then dried using a critical point dryer.²⁷ The test microstructures are in the form of solid cubes of varied dimensions printed with identical writing parameters. The substrates investigated in this study are used either in their pristine form or after modification with an adhesion promoter. In their pristine form, prior to printing, the glass coverslips are washed in acetone and isopropanol and then air-dried. In their modified form, the glass coverslips are first cleaned by immersing them in an oxidizing solution made of sulfuric acid and hydrogen peroxide (3:1 volume ratio) for 30 min. The substrates are then washed thoroughly with deionized water, and after being dried, they are placed in a low-vacuum chamber with 3 ml of 3-acryloxy propyl trichlorosilane (Gelest, Inc.) for 2 h. During this time, the hydroxyl functional groups present on the surface of the freshly oxidized glass substrate react with the silane agent releasing hydrochloric acid and forming a monolayer of acrylic functional groups covalently linked to the glass surface.²⁸

III. RESULTS AND DISCUSSION

A qualitative example of the adhesion properties' differences between the unmodified and modified glass substrates is shown in Fig. 1. In both substrates, an array of test samples is written by TPP where all the cubes have the same dimensions (30 μm side length). Although the entire sets of microstructures in the arrays survive the

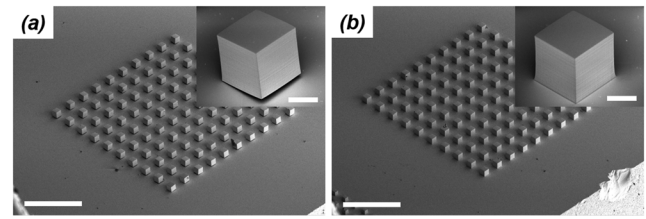


FIG. 1. SEM images of microstructures fabricated by TPP-DLW on glass substrates with and without an adhesion promoter. All polymeric specimens are made at a writing speed of 2 cm/s using lateral and axial hatching values of 100 nm and 200 nm, respectively. The laser average power during the writing is set to 17 mW. (a) When using an unmodified glass substrate, TPP microstructures remain attached to the glass surface, but they all show adhesion defects due to shrinkage induced stresses within the polymer. The inset is a magnified view of one of the test samples, showing clearly how faulty is the polymer-glass interface. (b) When a glass substrate modified with an adhesion promoter is used instead, TPP microstructures are all firmly anchored to the glass surface. Furthermore, the polymer-glass interface remains completely sealed (inset) showing the absence of any gaps. The scale bars in both images are 250 μm. The scale bars in both inset images are 20 μm.

washing and drying step, a closer look at their interface with the glass substrate reveals a different story. While the base of the printed cube is firmly attached to the substrate with the modified surface [inset of Fig. 1(b)], a clear gap between the polymer microstructure and the glass substrate is visible in the case of the pristine unmodified substrate [inset of Fig. 1(a)]. Upon polymerization, acrylic-based resins used in TPP-DLW undergo a certain amount of shrinkage, which is unavoidable since it is a direct consequence of the chemical process that creates the stiff and self-supported material required for 3D printing.²⁹ The results in Fig. 1(a) point to the fact that the shrinkage-induced stresses that develop within a printed part in TPP-DLW are of sufficient magnitude to overcome the fracture energy of the interface, which is related to the adhesion force that keeps the microstructures attached to the pristine substrate.

To quantify these forces and measure the adhesion enhancement observed with the modified glass substrates [Fig. 1(b)], we perform force-position measurements on TPP specimens similar to the ones shown in Fig. 1 by means of a MEMS-based force-sensing probe system (FemtoTools AG). The sensing probe (FT-S200) employed in the setup is calibrated to measure forces from nN to mN. The polymeric samples are tested by applying a shear displacement. Specifically, the side face of each cube is pushed with increasing displacement until the cube itself is dislodged from the substrate. The direction of the applied displacement is normal to the cube side and parallel to the substrate. An image recorded with an optical microscope in reflective mode showing the force-sensing probe pushing on one of the TPP microstructures is shown in the inset of Fig. 2(a).

The force-displacement curves obtained from microstructures attached to the unmodified glass substrates are considerably different from the ones obtained from microstructures attached to the modified glass substrates. Representative curves that underscore this difference are shown in Fig. 2(a), where polymeric cubes with side lengths of 10 μm are tested. As expected, no significant force is measured before contact between the polymeric cubes, and the

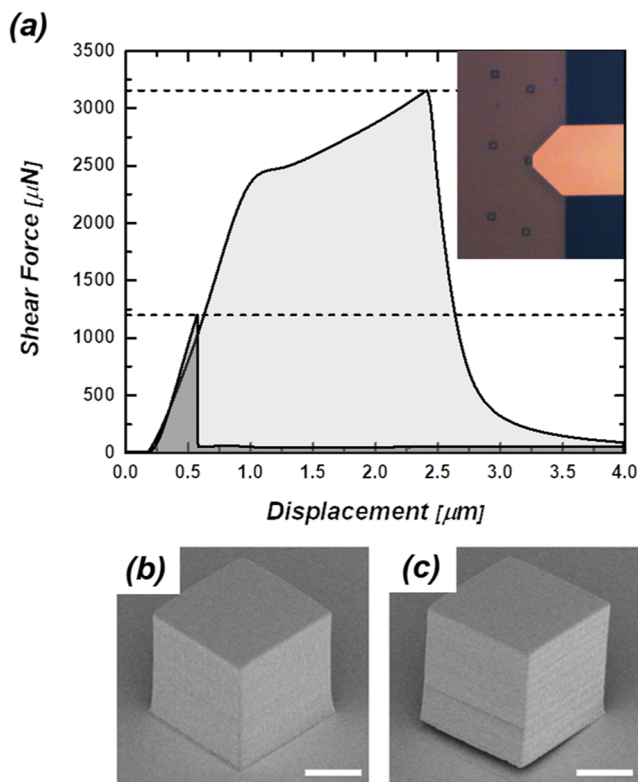


FIG. 2. (a) Shear force measurements of polymeric cubes fabricated by TPP-DLW on unmodified (dark shade gray plot) and modified (light gray shade plot) glass substrates. In both cases, cubes of side lengths of $10\ \mu\text{m}$ are tested. The horizontal dashed lines identify the force maxima required to dislodge the microstructures from the substrates. Light microscopy image of a force–displacement experiment conducted on a cube with a side length of $30\ \mu\text{m}$ is shown in the inset. The force sensor is the bright trapezoidal structure on the right of the image. Post-mortem SEM images of TPP microstructures fabricated on unmodified (b) and modified (c) substrates. A clear sign of plastic deformation due to the contact with the force sensor is visible only on the microstructure fabricated on the modified substrate. The scale bars in (b) and (c) are $5\ \mu\text{m}$.

MEMS-based probe occurs. In the instance of an unmodified glass substrate (dark gray shade), as soon as contact is engaged, the applied force increases rapidly with the minimum displacement of the probe. When the applied force exceeds the adhesion force between polymer and glass, the probe begins again to measure displacement with virtually no force. This is because the microstructure is no longer anchored to the substrate.

The force required to detach the TPP microstructure from the unmodified glass is the maximum shear force, which in this case measures around $1200\ \mu\text{N}$ (dashed horizontal line). When a cube is attached to a modified glass substrate, a considerable increase in the maximum shear force ($\sim 3200\ \mu\text{N}$) is observed instead (light gray shade). This result can be explained by the stronger adhesion between the polymer and the substrate due to the silane coupling agent used to modify the glass surface.³⁰ Besides the disparity in shear force maxima, the evolution of the force–displacement curves is quite different between the two samples. The work needed to

remove the polymeric cube from the modified substrate (i.e., the area under the force–displacement curve) is considerably larger than the work needed for the same job on an unmodified substrate. Furthermore, while the polymeric cube on the unmodified substrate remains elastic throughout the deformation and separates from the substrate in a brittle manner (as indicated by the vertical slope of the load drop in the load–displacement curve), the polymeric cube attached to the modified substrate undergoes plastic deformation before being detached from the substrate, as shown by the change in slope (stiffness) in the force–displacement curve at a force of $\sim 2500\ \mu\text{N}$. Assuming a uniform shear stress across the sample and a sample area of $100\ \mu\text{m}^2$, this corresponds to a yield strength in shear of $F/A = 25\ \text{MPa}$. Using the simple Von Mises yield criterion,³¹ this number gives a yield strength in compression of $\sigma_y = \sqrt{3}\tau_y = 43\ \text{MPa}$. This value is of the same order of magnitude as that reported by Bauer *et al.* for the same material,³² indicating that the test setup reasonably approximates a pure shear test. The same sample also shows evidence of ductile fracture from the substrate, as indicated by the negative slope of the load drop in the force–displacement curve. In agreement with these findings, post-mortem analysis of the polymeric cubes, using SEM [Figs. 2(b) and 2(c)], reveals that microstructures on the unmodified substrate maintain the initial shape, while microstructures on the modified substrate present permanent deformation.

At the length scales involved in TPP-DLW, the surface of the substrates can be considered smooth and chemically homogeneous. Consequentially, the adhesion of polymeric microstructures to glass slides is expected to scale linearly with the size of the contact area. To prove this assumption, we have fabricated a series of polymer cubes by TPP-DLW ranging in side lengths from $7.5\ \mu\text{m}$ to $50\ \mu\text{m}$ on the modified and unmodified substrates. Using the methodology described earlier, we have measured the maximum shear force needed to dislodge the microstructures from the glass slides. The results are summarized in Fig. 3, where this value is now named the adhesion force. For both substrates, a growth in adhesion force is observed as the size of the polymer structure increases. Independently of their size, microstructures printed on the modified substrate are all attached to the glass slide with a stronger bond compared to microstructures printed on the unmodified substrate. Interestingly, the data in Fig. 3 follow a linear relationship (continuous line) for smaller polymeric cubes only. As the microstructures grow in size, a negative deviation of the shear force maxima from the linear dependence is observed for both substrates. Taken together, the data follow a simple power function (dashed line) of the form $y = a\sqrt[n]{x}$, where the power coefficient n determines the rate at which the shear force maxima decrease with growing cube sizes.

This behavior indicates a decrease in the average interface strength as the sample size is increased and can be attributed to the presence of imperfections (nano-cracks).³³ In the particular case of TPP microstructures printed on glass surfaces, two phenomena contribute to the presence of nano-cracks. The first one is the less-than-ideal conformal contact at the interface due to the line-by-line writing method used to build the parts. The second one is the shrinkage-induced stress that follows the radical polymerization of acrylic-based resins such as IP-Dip.²⁹ These nano-cracks have the overall effect of decreasing the area that the polymeric microstructure shares in contact with the substrate, i.e., the effective

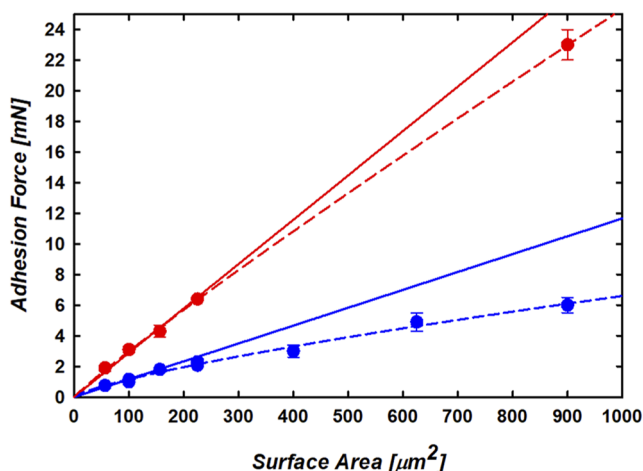


FIG. 3. Dependence of the adhesion force (see text for definition) between TPP microstructures and the glass substrates as a function of the contact area. Data from the modified and unmodified glass slides are displayed in red and blue, respectively. The continuous lines are linear regressions that use solely the first three data points corresponding to cube microstructures with sizes of 7.5 μm , 10 μm , and 12.5 μm . The dashed lines are regressions of all the data based on a power function.

contact area with the glass slide is smaller than the one obtained by the microstructure's dimensions. The aforementioned causes of the nano-cracks are dependent on the size of the polymeric microstructure area in contact with the substrate. Therefore, both the density of the nano-cracks and their propagation during the shear stress tests are proportional to the size of the microstructure.

Figure 3 provides two numbers that quantify the amelioration of TPP microstructures' bonding to glass when using an adhesion promoter. For small objects, the impact of nano-cracks on adhesion is negligible, and the slopes of the linear regressions provide the force per unit area required to detach the polymeric microstructures, i.e., the average strength of the interface. For the modified and unmodified substrates, these numbers are 29 $\mu\text{N}/\mu\text{m}^2$ and 12 $\mu\text{N}/\mu\text{m}^2$, respectively. This sizable improvement clearly explains the results shown in Fig. 1. As the printed objects become larger, the effect of the nano-cracks on adhesion cannot be ignored anymore. Nonetheless, the rate at which the experimental data deviate from the expected linear behavior is larger for the unmodified substrate than for the modified one. Specifically, the power coefficient n is 1.32 and 1.08 for the pristine glass and the glass modified with the silane agent, respectively. Thus, the adhesion promoter used in the modified substrates offsets the detrimental effect, and the polymer shrinkage-induced stresses inflict on the ultimate bonding between the microstructures and the substrate.

The experimental data presented so far establish that the adhesion of TPP microstructures to glass substrates can be enhanced by using a silane coupling agent. To understand the mechanism by which this enhancement occurs, the different types of forces that play a role in bond creation at the interface must be examined.³⁴ For this reason, we have determined the surface free energy (γ) of both the unmodified and modified glass substrates by means of a contact

angle goniometer (Attension Theta Lite, Biolin Scientific). Values of γ for the different substrates are obtained at room temperature by measuring the contact angles of test liquids whose surface tensions are known (water and diiodomethane) and fitting the results using the OWRK/Fowkes model.³⁵ The measurements reveal similar surface free energies for the unmodified and modified glass substrates. Specifically, $\gamma_{\text{unmodified}} = 45.1 \text{ mN/m}$ and $\gamma_{\text{modified}} = 49.5 \text{ mN/m}$. Since the surface tension of IP-Dip is 37.7 mN/m, these results establish that a thermodynamic mechanism is not adequate to explain the observed enhancement in adhesion. Moreover, if only dispersive and polar interactions were used to describe the thermodynamics of adhesion,³⁶ then a result opposite to the one measured would be expected since $\gamma_{\text{unmodified}}$ is closer to the resin's surface tension than γ_{modified} .

Based on this finding, we propose that the main contributor to the observed adhesion enhancement of TPP microstructures on glass substrates is the formation of covalent bonds between the polymer and the substrate itself that occur during the photopolymerization process. This is possible because of the acrylic moieties that are added to the glass surface upon its modification. In essence, the silanization of the glass surface creates a chemical bridging between the polymeric microstructure and the inorganic substrate. Although spectroscopic studies will have to be implemented to experimentally verify this hypothesis, a simple calculation can be used to corroborate this scenario. The energy necessary to detach a microstructure from the substrate is simply the integration of its force/displacement curve (Fig. 2). For a polymer cube with a size of 10 μm printed on a modified glass substrate, an energy of $6 \times 10^{-12} \text{ kJ}$ is found. The density of hydroxyl groups for a glass surface is $\sim 7/\text{nm}^2$.³⁷ Considering that during surface modification every acrylic moiety is linked to three hydroxyl groups and that the Si-O bond has a strength of 452 kJ/mol, the energy required to detach a polymeric cube with a size of 10 μm printed on a modified glass substrate is calculated to be $2 \times 10^{-12} \text{ kJ}$. The measured and calculated energies are of same order of magnitude (assuming that the chemical bond broken during the detachment of the two parts is the Si-O one between the silane coupling agent and the glass surface). Furthermore, the larger value for the measured energy can be explained by taking into consideration that some of the shear force is damped by the microstructure through elastic deformation.

To demonstrate the impact that surface modification of substrates can have on the survivability of microstructures made by TPP-DLW, we have performed a comparison among microstructures printed on the modified and unmodified substrates after they underwent pyrolysis. During pyrolysis, polymeric microstructures are thermally decomposed in vacuum at temperatures in the range of 1000–3000 $^{\circ}\text{C}$. The result is the transformation of the acrylic-based material into a disordered carbon allotrope known as glassy-carbon. Hence, by means of TPP-DLW and subsequent pyrolysis, microstructures with significantly enhanced physical properties can be obtained.²² The formation of glassy-carbon microstructures is accompanied by an isotropic volume shrinkage that can reach values as high as 90%. Although this effect is exploited in TPP-DLW to create ultralight microstructures with sub-100 nm feature sizes, it also causes the delamination of the parts from their substrates. That is, during pyrolysis, microstructures tend to detach from the substrates because of the shrinkage-induced stresses that are very asymmetric

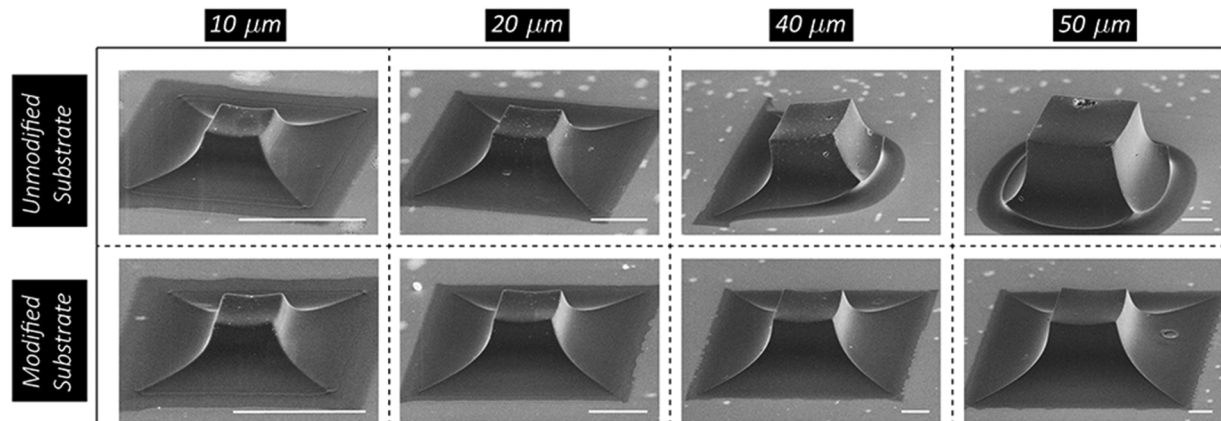


FIG. 4. SEM images of microstructures fabricated by TPP-DLW followed by pyrolysis. Each column is defined by the size of the original cube side length. The two rows correspond to microstructures printed on the unmodified and modified substrates. The images were taken at different magnifications. The scale bar is $5\ \mu\text{m}$ for all the images.

at the polymer/substrate interface. The SEM images in Fig. 4 prove that the surface modification of TPP-DLW substrates described earlier has a positive effect on the ability of TPP microstructures to survive pyrolysis as well. Four test cubes are printed on the unmodified and modified substrates.

All print jobs are carried out using the same experimental conditions; the only difference is the overall size. Cubes with side lengths of $10\ \mu\text{m}$, $20\ \mu\text{m}$, $40\ \mu\text{m}$, and $50\ \mu\text{m}$ are tested. The side of the polymeric cube that is in contact with the substrate experiences an amount of shrinkage during pyrolysis that is much smaller than what is experienced by the rest of the polymeric cube, thus explaining the shapes of the microstructures shown in Fig. 4. While microstructures larger than $20\ \mu\text{m}$ all fail (detach from the substrate) during pyrolysis in the case of unmodified substrates, microstructures with a base as large as $50\ \mu\text{m}$ remain intact during pyrolysis when printed on the modified substrates.

IV. SUMMARY

In summary, we present a method to quantitatively measure the forces involved in the adhesion of microstructures fabricated by TPP-DLW to glass substrates. This methodology is used to compare the adhesion between pristine glass substrates and substrates modified with a coupling silane agent. A prominent adhesion enhancement is observed and measured. Furthermore, the results found in this study are applied to TPP microstructures that are turned into glassy-carbon microstructures via pyrolysis. The results in Fig. 4 are promising for overcoming shrinking of TPP-DLW parts following pyrolysis, possibly offering an approach for the fabrication of larger mechanical metamaterials.

ACKNOWLEDGMENTS

The authors acknowledge financial support from the NSF under Grant No. CMMI-1905582.

The data that support the findings of this study are available within the article.

REFERENCES

- S. Maruo and J. T. Fourkas, *Laser Photonics Rev.* **2**(1-2), 100 (2008).
- M. Malinauskas, M. Farsari, A. Piskarskas, and S. Juodkazis, *Phys. Rep.* **533**(1), 1 (2013).
- K.-S. Lee, R. H. Kim, D.-Y. Yang, and S. H. Park, *Prog. Polym. Sci.* **33**(6), 631 (2008).
- C. W. Ha, P. Prabhakaran, and K.-S. Lee, *MRS Commun.* **9**(1), 53 (2019).
- S. Kawata, H.-B. Sun, T. Tanaka, and K. Takada, *Nature* **412**(6848), 697 (2001).
- J. Serbin, A. Egbert, A. Ostendorf, B. N. Chichkov, R. Houbertz, G. Domann, J. Schulz, C. Cronauer, L. Fröhlich, and M. Popall, *Opt. Lett.* **28**(5), 301 (2003).
- T. Ergin, N. Stenger, P. Brenner, J. B. Pendry, and M. Wegener, *Science* **328**(5976), 337 (2010).
- J. Bauer, L. R. Meza, T. A. Schaedler, R. Schwaiger, X. Y. Zheng, and L. Valdevit, *Adv. Mater.* **29**(40), 1701850 (2017).
- T. Buckmann, M. Thiel, M. Kadic, R. Schittny, and M. Wegener, *Nat. Commun.* **5**, 4130 (2014).
- A. Ovsianikov, S. Mühleder, J. Torgersen, Z. Q. Li, X.-H. Qin, S. Van Vlierberghe, P. Dubruel, W. Holthöner, H. Redl, R. Liska, and J. Stampfl, *Langmuir* **30**(13), 3787 (2014).
- P. Tayalia, C. R. Mendonca, T. Baldacchini, D. J. Mooney, and E. Mazur, *Adv. Mater.* **20**(23), 4494 (2008).
- A. K. Nguyen and R. J. Narayan, *Mater. Today* **20**(6), 314 (2017).
- M. T. Raimondi, S. M. Eaton, M. M. Nava, M. Laganà, G. Cerullo, and R. Osellame, *J. Appl. Biomater. Funct. Mater.* **10**(1), 56 (2012).
- S. D. Gittard, A. Nguyen, K. Obata, A. Koroleva, R. J. Narayan, and B. N. Chichkov, *Biomed. Opt. Express* **2**(11), 3167 (2011).
- L. Kelemen, E. Lepera, B. Horváth, P. Ormos, R. Osellame, and R. M. Vazquez, *Lab Chip* **19**(11), 1985 (2019).
- S. Maruo and H. Inoue, *Appl. Phys. Lett.* **89**(14), 144101 (2006).
- G. Kumi, C. O. Yanez, K. D. Belfield, and J. T. Fourkas, *Lab Chip* **10**(8), 1057 (2010).
- J. T. Fourkas, *Fundamentals of Two-Photon Fabrication* (Elsevier, New York, 2016), p. 45.
- L. Jonusauskas, D. Gailevicius, S. Rekstyte, T. Baldacchini, S. Juodkazis, and M. Malinauskas, *Opt. Express* **27**(11), 15205 (2019).
- V. Hahn, P. Kiefer, T. Frenzel, J. Y. Qu, E. Blasco, C. Barner-Kowollik, and M. Wegener, "Rapid assembly of small materials building blocks (Voxels) into large functional 3D metamaterials," *Adv. Funct. Mater.* (published online, 2020).
- M. Kadic, T. Buckmann, R. Schittny, and M. Wegener, *Rep. Prog. Phys.* **76**(12), 126501 (2013).

- ²²J. Bauer, A. Schroer, R. Schwaiger, and O. Kraft, *Nat. Mater.* **15**(4), 438 (2016).
- ²³X. Zhang, A. Vyatskikh, H. J. Gao, J. R. Greer, and X. Y. Li, *Proc. Natl. Acad. Sci. U. S. A.* **116**(14), 6665 (2019).
- ²⁴C. Barner-Kowollik, M. Bastmeyer, E. Blasco, G. Delaittre, P. Müller, B. Richter, and M. Wegener, *Angew. Chem., Int. Ed.* **56**(50), 15828 (2017).
- ²⁵C. N. LaFratta and T. Baldacchini, *Micromachines* **8**(4), 101 (2017).
- ²⁶T. Bückmann, N. Stenger, M. Kadic, J. Kaschke, A. Frölich, T. Kennerknecht, C. Eberl, M. Thiel, and M. Wegener, *Adv. Mater.* **24**(20), 2710 (2012).
- ²⁷S. Maruo, T. Hasegawa, and N. Yoshimura, *Opt. Express* **17**(23), 20945 (2009).
- ²⁸H. L. Cong and T. R. Pan, *Adv. Funct. Mater.* **18**(13), 1912 (2008).
- ²⁹C. L. Davidson and A. J. Feilzer, *J. Dent.* **25**(6), 435 (1997).
- ³⁰E. P. Plueddemann, *Prog. Org. Coat.* **11**(3), 297 (1983).
- ³¹W. H. Yang, *J. Appl. Mech.* **47**(2), 297 (1980).
- ³²J. Bauer, A. G. Izard, Y. F. Zhang, T. Baldacchini, and L. Valdevit, *Adv. Mater. Technol.* **4**(9), 1900146 (2019).
- ³³W. P. Vellinga, R. Timmerman, R. van Tijing, and J. T. M. De Hosson, *Appl. Phys. Lett.* **88**(6), 061912 (2006).
- ³⁴F. Awaja, M. Gilbert, G. Kelly, B. Fox, and P. J. Pigram, *Prog. Polym. Sci.* **34**(9), 948 (2009).
- ³⁵M. Lewin, A. Mey-Marom, and R. Frank, *Polym. Adv. Technol.* **16**(6), 429 (2005).
- ³⁶G. Fourche, *Polym. Eng. Sci.* **35**(12), 957 (1995).
- ³⁷L. T. Zhuravlev, *Langmuir* **3**(3), 316 (1987).